Electronic Supplementary Material (ESI) for Journal of Materials Chemistry A.

Contents

1. Materials Preparation 2
  1.1. Materials 2
  1.2. Synthesis of Zn_2(dobdc) 2
  1.3. Preparation of EDT and nPM loaded samples 2
2. Powder X-ray Diffraction 3
  2.1. Data Collection 3
  2.2. Structural Analysis of MeOH-Solvated Zn_2(dobdc) 3
  2.3. Structural Analysis of nPM-Loaded Zn_2(dobdc) 3
3. Infrared Spectroscopy 8
4. Thermogravimetric Measurements 8
5. Porosity Measurements 8
6. Scanning Electron Microscopy 9
7. Theoretical Calculations 10
8. Photoluminescence Spectroscopy 13
9. Fluorescence Microscopy 13
  9.1. Gradual loading 13
  9.2. Cation Sensing Screening 14
References 16

1. Materials Preparation

1.1. Materials

N,*N*-dimethylformamide, methanol, and potassium carbonate were purchased from Fisher and used as received. Cobalt nitrate hexahydrate, zinc nitrate hexahydrate, hydroquinone, formic acid and *n*-propylmercaptan (nPM) were purchased from Alfa Aesar and used as received. 1,2-Ethanedithiol (EDT) was purchased from TCI and used as received. Ethanol was purchased from Sigma Aldrich and used as received. 2,5-Dihydroxyterephthalic acid was synthesized using a procedure from the literature.[1]

1.2. Synthesis of Zn_2(dobdc)

The material Zn_2(dobdc) was synthesized following the literature;[2] 2,5-dihydroxyterephthalic acid (2.00 g, 10.1 mmol) and zinc nitrate hexahydrate (8.00 g, 26.9 mmol) were transferred to a 1 L pressure bottle and dissolved in 400 mL of DMF, which had been degassed with nitrogen. The solids were dissolved, then 25 mL of degassed, deionized water was added and the bottle placed into a 100 °C oven for 24 h. The red-orange supernatant was decanted and the yellow-green crystals were soaked in approximately 200 mL of DMF for 8+ hours before decanting and replacing the solvent. After two more DMF soaks following the same procedure, methanol was added and the bottle placed into a 60 °C oven for 8+ hours. After two more methanol soaks following the same procedure, the solid was filtered and dried on the benchtop. PXRD analysis confirmed that the product is a single-phase, highly crystalline, MeOH-solvated Zn_2(dobdc). The vial was then transferred to a glovebox for storage.

Synthesis of highly porous Zn_2(dobdc). In order to reliably prepare highly porous Zn_2(dobdc) on large scale, an alternative procedure was employed to produce microcrystalline material.1 A 350 mL screw-cap high pressure reaction vessel equipped with a stir bar was charged with $Zn(NO_3)_2{\cdot}{}_6H_2O$ (2.23 g, 7.50 mmol, 3.00 eq.), H_4dobdc (495 mg, 2.50 mmol, 1.00 eq.), fresh DMF (125 mL), and ethanol (125 mL). The mixture was sonicated until all of the solids dissolved. The reaction mixture was vigorously sparged with N_2 for 1 h. The reaction vessel was sealed, and the reaction mixture was allowed to stir slowly at 120 °C for 14 h, resulting in precipitation of a yellow powder from solution. The reaction mixture was cooled to room temperature and filtered. The collected solid was quickly transferred to a 500 mL Pyrex jar filled with DMF (250 mL). The jar was placed in an oven that had been pre-heated to 120 °C and left to stand for 24 h, after which time the non-homogeneous mixture was filtered. The collected solid was returned to the jar with fresh DMF (250 mL) and returned to an oven that had been pre-heated to 120 °C. This soaking process was repeated for a total of three hot DMF soaks. The mixture was then filtered and transferred to a 500 mL Pyrex jar filled with methanol (250 mL), and the jar was placed in an oven that had been pre-heated to 60 °C and left to stand 24 h, after which time the non-homogeneous mixture was filtered. The collected solid was returned to the jar with fresh methanol (250 mL) and returned to an oven that had been pre-heated to 60 °C. This soaking process was repeated for a total of three hot methanol soaks. The mixture was filtered a final time, and the collected solid was quickly transferred to a 50 mL Schlenk flask. The material was activated under high vacuum (<100 mTorr) at 180 °C for 24 h. The Schlenk flask was transferred into a N2-filled glovebox, and the dark yellow solid was transferred to a 20 mL scintillation vial for storage. A portion (~100 mg) of the activated Zn2(dobdc) was transferred to a glass adsorption tube equipped with a Micromeritics CheckSeal. The tube was removed from the glovebox and the material was activated for an additional 24 h under high vacuum (<10 μbar) at 180 °C prior to gas adsorption experiments. This procedure was repeated twice to prepare two separate batches of Zn2(dobdc) for this work.

1.3. Preparation of EDT and nPM loaded samples

For the preparation of the EDT- and nPM-loaded samples, ~100 mg of MeOH-solvated Zn_2(dobdc) was transferred to 20 mL vials. The mmol of Zn^{2+} in each vial was calculated using the methanol-solvated formula, $Zn_2(dobdc)(MeOH)_2$. Methanol solutions of both 0.1 M EDT and 0.1 M nPM were prepared. The convention for loading was based on the open zinc-sites. Using EDT as an example, 100 mol% of EDT per Zn, which correlates to 200% mol% of EDT per MOF. Each sample was prepared by first adding methanol, for dilution, followed by the corresponding amount of EDT or nPM solution. Methanol and the solution were added such that the total volume equaled 20 mL/mmol MOF, which meant a maximum concentration of 0.1 M nPM or EDT. For the 100% loading, the 0.1 M solution were added without dilution. The samples were soaked for 20 h, while being agitated several times. Finally, the samples were decanted and soaked in methanol for 30 minutes before collection by vacuum filtration. The samples were dried under air and characterized using PXRD to assess their crystallinity.

Loadings of 500% were obtained following a similar method, but using 0.5 M nPM and EDT methanolic solutions, without dilution.

2. Powder X-ray Diffraction

2.1. Data Collection

Powder X-ray diffraction (PXRD) data was collected on a laboratory Stoe Stadi-P powder diffractometer, operating in Debye−Scherrer geometry. The diffractometer was equipped with a molybdenum X-ray source and monochromatic Mo-Kα1 radiation (λ = 0.709 30 Å) obtained by a primary Ge(111) monochromator. The goniometer had 2 circles (140 mm and 80 mm). Two linear position sensitive silicon-strip (Mythen Dectris 1K, 50 µm step size) detectors were used to record the scattered X-ray intensity. The instrumental parameters for the diffractometer were refined against LnB6 NIST standard. Before data collection, each sample was dried under an inert atmosphere and densely packed in a borosilicate capillary (0.5 mm diameter). Diffraction data was collected at room temperature. The capillary was rotated for better particle statistics during the measurements. Diffraction data used for crystal structure solution and refinement was collected for 24 h within the complete range of the two 1K detectors. Diffraction data for assessing the crystallinity and/or phase purity of the samples was collected for 1h.

2.2. Structural Analysis of MeOH-Solvated Zn_2(dobdc)

The PXRD pattern of the MeOH-solvated Zn_2(dobdc), which was used for the majority of the experiments, was analyzed with the software TOPAS-Academic V6.[4] Precise unit cell parameters were obtained by Pawley fitting.[5] The crystal structure was solved by the real-space global optimization simulated annealing (SA) method,[6] using the published model of the activated Zn_2(dobdc) crystal structure as a starting model. Once the SA optimization converged to a global minimum, the structure was subjected to Rietveld refinement.[7] During the refinement, the following parameters were set free: unit cell and peak profile parameters, background coefficients (described as a Chebyshev polynomial), site occupancies, fractional coordinates of two methanol molecules, fractional coordinates of the Zn cation, and thermal displacement parameters defined as a single variable for each atomic type. The Rietveld plot is given in Figure S1, fraction of the crystal structure is given in Figure S2, and selected crystallographic and structural data are given in Table S1. A CIF of the structure is included as supplementary information.

2.3. Structural Analysis of nPM-Loaded Zn_2(dobdc)

The PXRD pattern of the nPM-loaded Zn_2(dobdc) was analyzed with the software TOPAS-Academic V6.[4] Precise unit cell parameters were obtained by Pawley fitting.[5] The crystal structure was solved by the real-space global optimization simulated annealing (SA) method,[6] using the published model of the activated Zn_2(dobdc) crystal structure as a starting model. Once the SA optimization converged to a global minimum, the structure was subjected to Rietveld refinement.[7] During the refinement, the following parameters were set free: unit cell and peak profile parameters, background coefficients (described as a Chebyshev polynomial), site occupancies, fractional coordinates of one nPM molecule, fractional coordinates of the Zn cation, and thermal displacement parameters defined as a single variable for each atomic type. The Rietveld plot is given in Figure S3, fraction of the crystal structure is given in Figure S4, and selected crystallographic and structural data are given in Table S1. A CIF of the structure is included as supplementary information.

Table S1. Selected experimental and structural parameters for the studied samples.

	MeOH-solvated Zn_2(dobdc)	nPM-loaded Zn_2(dobdc)
λ (Å)	0.709 30	0.709 30
Temperature (K)	298	298
2θ range (°)	1 – 45	1 – 45
Time (h)	24	24
Crystal system	Rhombohedral	Rhombohedral
Space Group	$R\overline{3}$	$R\overline{3}$
a (Å)	26.2100(6)	25.9208(11)
c (Å)	6.6177(3)	6.8681(7)
V (Å^3)	3937.0(2)	3937.0(2)
R_{wp} (%)[a]	7.69	6.14
R_{exp} (%)[a]	0.58	4.56
R_p (%)[a]	5.48	0.59
No. variables	35	43

[a] The figures of merit are as defined in TOPAS-Academic V6.

A close inspection of the difference curve in the Rietveld refinement of the nPM-loaded Zn_2(dobdc) presented in Figure S3 revealed additional reflections in the pattern that cannot be accounted for by the unit cell and symmetry of MOF-74. Similar reflections are present in the reported crystal structure of Co_2(dobdc) loaded with *o*-xylene adsorbates, solved by single crystal diffraction.[8] These reflections are characteristic of a doubling of the unit cell. These results indicate that the powder sample of nPM loaded Zn_2(dobdc) is a mixture of two crystalline phases: a major phase with the reported crystal structure, and a minor phase with lower symmetry and/or larger unit cell. We successfully refined the unit cell parameters using a two-phase Pawley fitting[5] with the usual MOF-74-unit cell parameters and an enlarged unit cell with $a = 52.157(3)$ Å and $b = 6.889(1)$ Å. The single phase and double phase Pawley fits are presented in Figure S5.

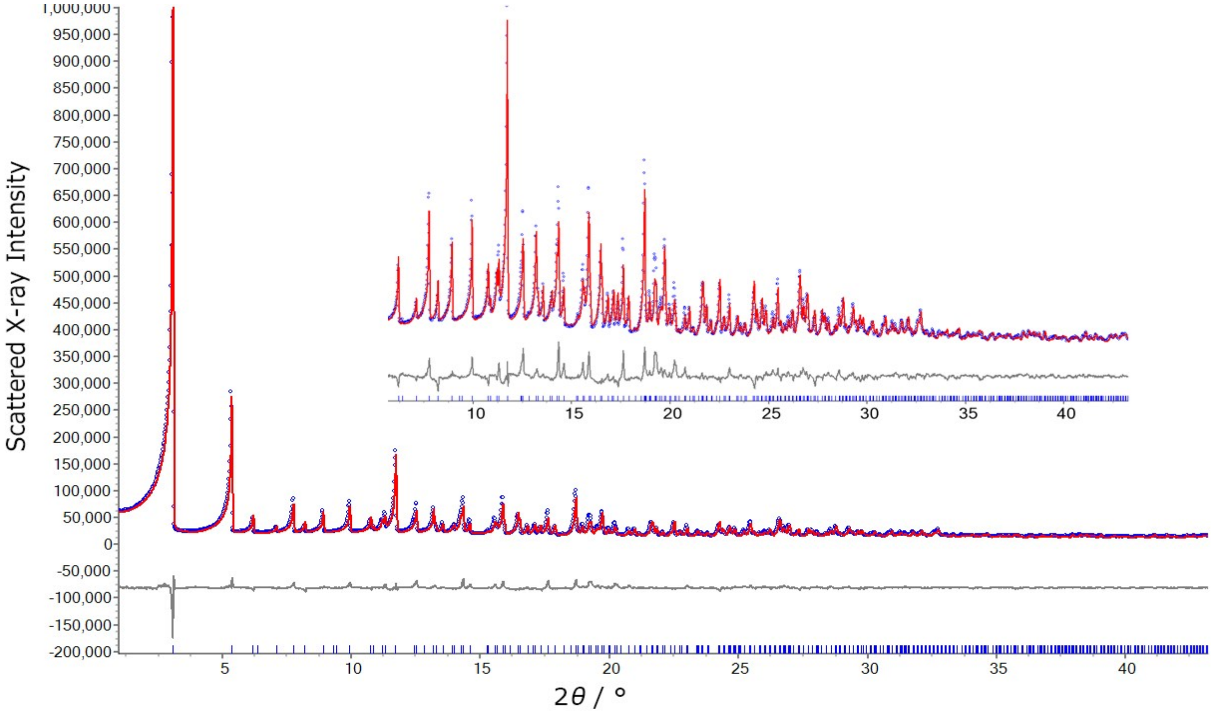

Figure S1. Powder diffraction pattern and Rietveld refinement plot for MeOH-solvated Zn_2(dobdc). Measured scattered X-ray intensity is presented as a blue line, the simulated pattern is presented as a red line, the difference curve between the measured and simulated patterns is presented as a gray line, and Bragg reflections are presented as blue bars.

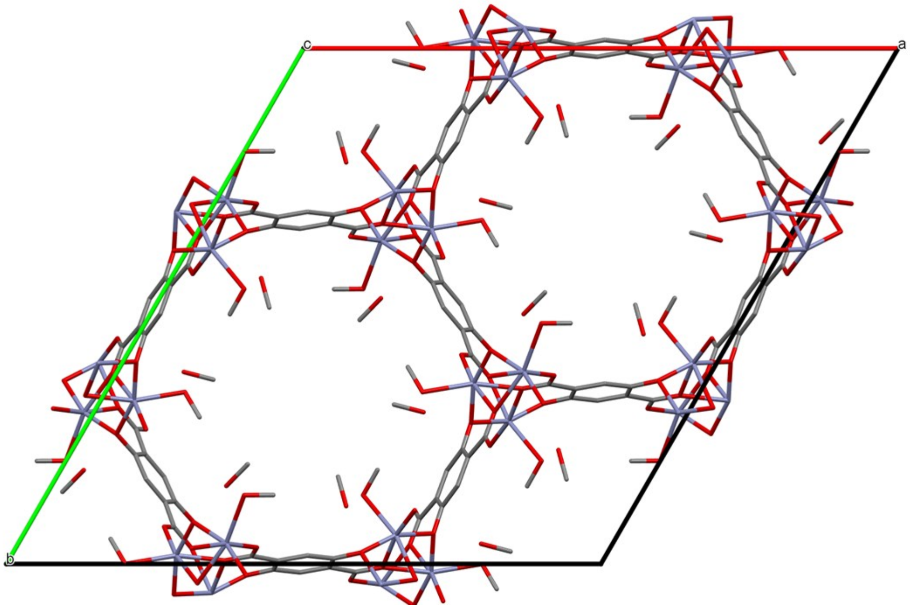

Figure S2. Fraction of the crystal structure of MeOH-solvated Zn_2(dobdc).

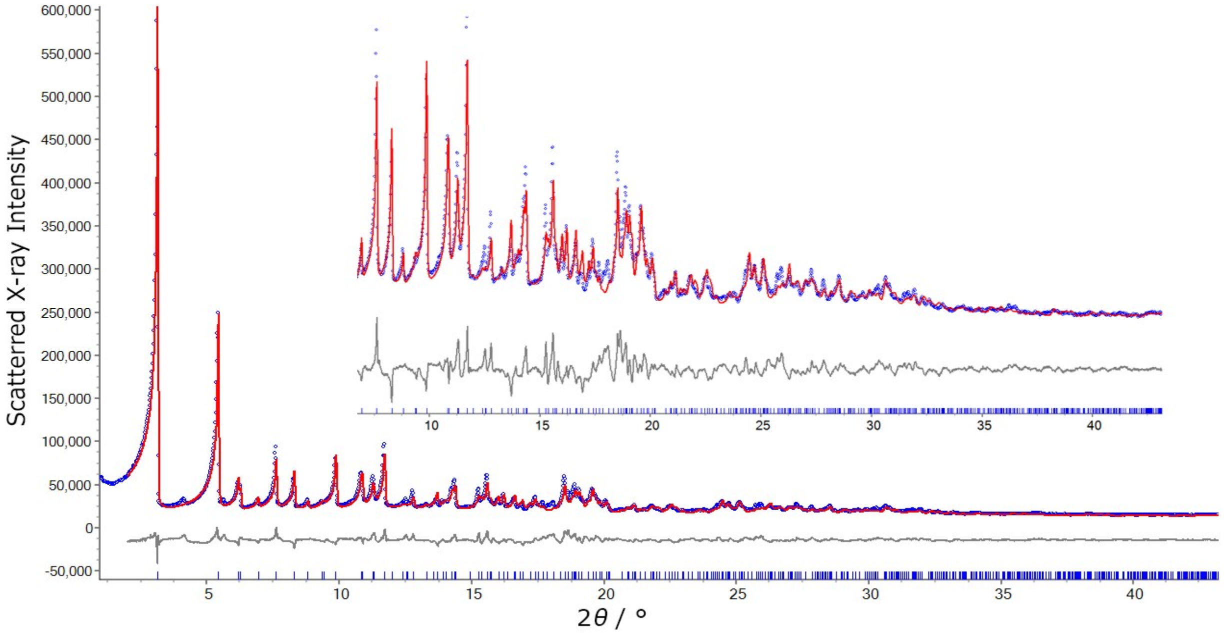

Figure S3. Powder diffraction pattern and Rietveld refinement plot for nPM-loaded Zn_2(dobdc). Measured scattered X-ray intensity is presented as a blue line, the simulated pattern is presented as a red line, the difference curve between the measured and simulated patterns is presented as a gray line, and Bragg reflections are presented as blue bars.

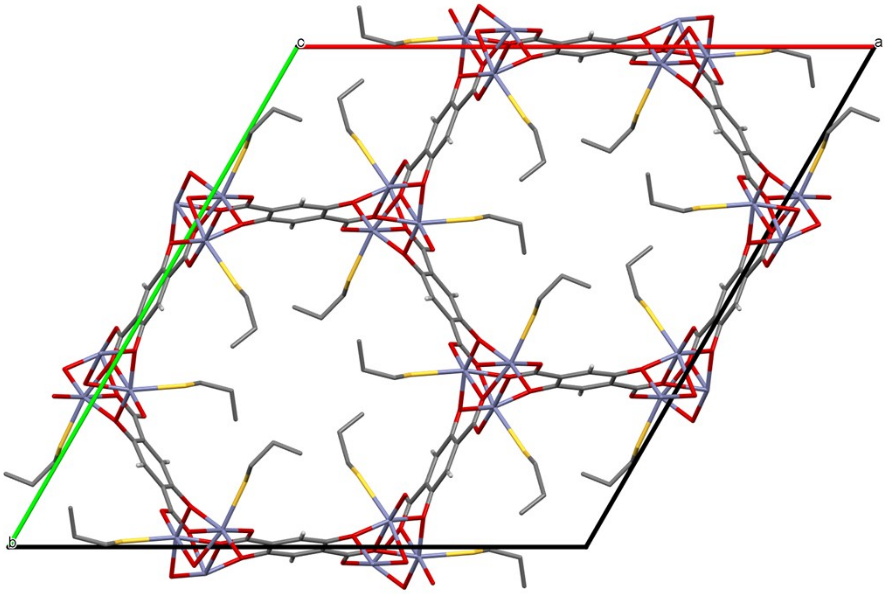

Figure S4. Fraction of the crystal structure of nPM-loaded Zn_2(dobdc).

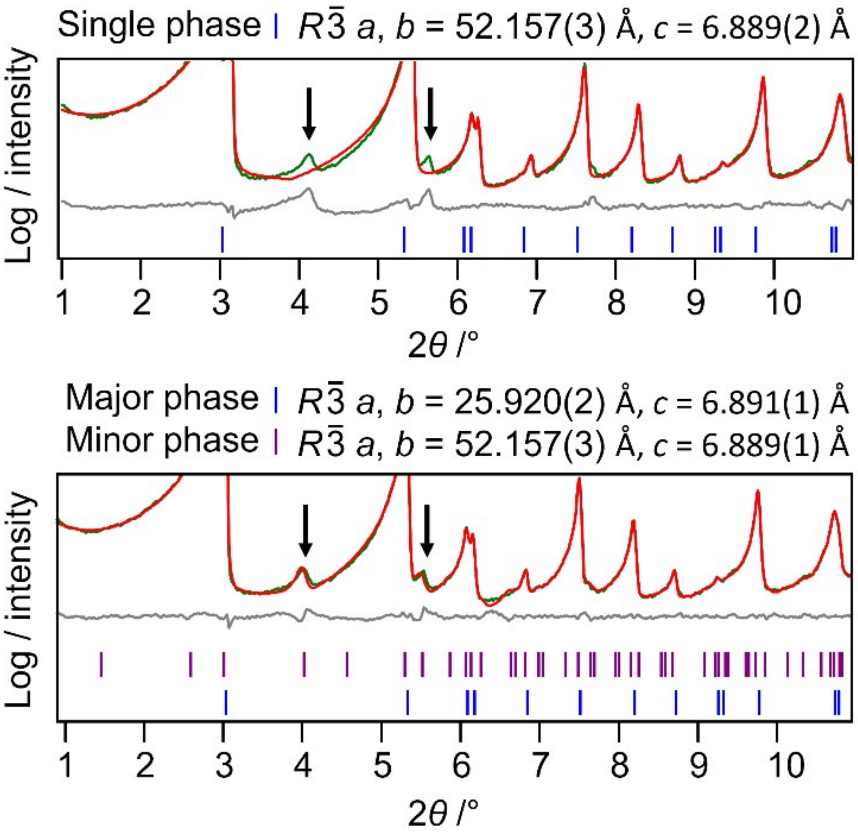

Figure S5. Top: Single-phase Pawley fitting of the diffraction data collected from nPM-loaded Zn_2(dobdc), using the same space group and starting unit cell parameters as for activated Zn_2(dobdc) (characteristic Bragg reflections presented as blue bars). Bottom: Double-phase Pawley fitting of the diffraction data collected from nPM-loaded Zn_2(dobdc), with a secondary phase described by a doubled b axis (characteristic Bragg reflections presented as purple bars).

3. Infrared Spectroscopy

Infrared spectra were collected with a Fourier transform infrared (FTIR) Thermo Fisher Nicolet iS50 spectrometer. The sample was ground, mixed with KBr powder, and pressed in a pellet. The infrared spectra of the gradually dosed samples are presented in Figure 2 in the main text.

4. Thermogravimetric Measurements

The thermogravimetric analysis (TGA) was performed with Netzsch TG 209 F3 Tarsus instrument. The samples were placed in an alumina crucible and heated from 298 to 1273 K, at heating a rate of 10 K/min, under a constant flow of nitrogen. The TG curves are presented in Figure 2 in the main text.

5. Porosity Measurements

Nitrogen adsorption/desorption isotherm for the activated sample of 0% EDT loaded Zn_2(dobdc) were measured at 77 K (Figure S6). The BET surface area was calculated to be 70.1 ± 0.2 m²/g. The activated samples of 60% EDT loaded Zn_2(dobdc) and 500% EDT loaded Zn_2(dobdc) were found to be nonporous. The three samples were activated on a Micromeritics SmartVac at 180 ºC for 48 hours under high vacuum (<10 µbar) and then activated for an additional 46 hours at 180ºC on a Micromeritics 3-flex gas sorption analyzer prior to analysis.

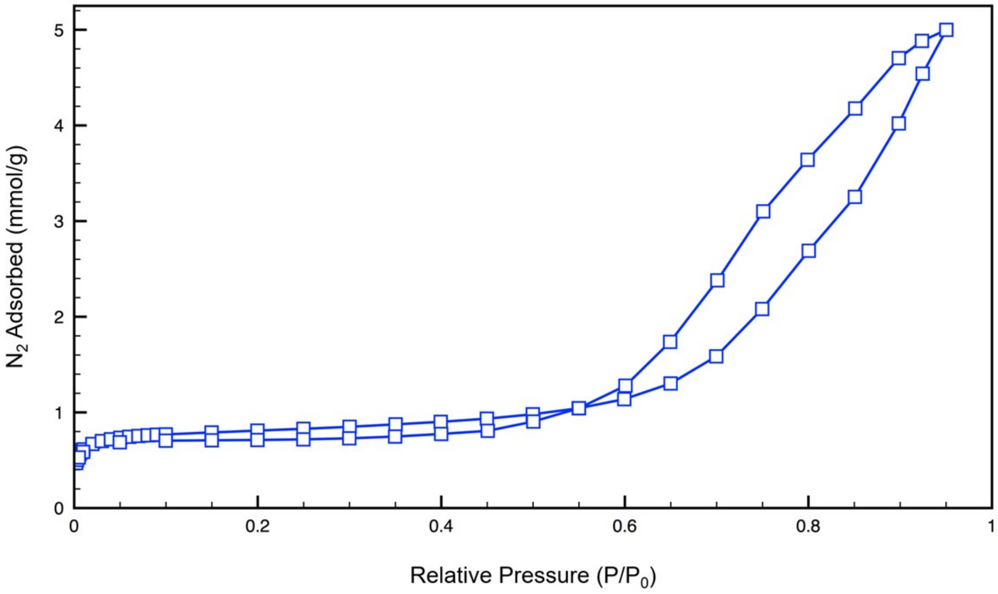

Figure S6. Nitrogen adsorption/desorption isotherm for the activated sample of 0% EDT-loaded Zn_2(dobdc) were measured at 77 K

Considering the low porosity of activated Zn_2(dobdc), we repeated the synthesis following a modified procedure, in order to obtain a highly porous sample (see section 1.2. for details). In a N_2-filled glovebox, three 20 mL scintillation vials were each charged with activated, highly porous Zn_2(dobdc) (97.5 mg, 0.30 mmol, 1.00 equiv.). The vials were capped and removed from the glovebox. Meanwhile, methanol (~15 mL) was vigorously sparged with N_2 for 30 min. At this time, a stock solution of 0.1 M EDT in methanol was prepared by adding EDT (41.9 µL, 0.50 mmol) to a 5 mL volumetric flask, which was then filled with degassed methanol. The vials were separately charged with 3.00 mL of the 0.1 M EDT solution (**100% EDT**), 0.30 mL of the 0.1 M EDT solution and 2.70 mL of degassed methanol (**10% EDT**), and 0.03 mL of the 0.1 M EDT solution and 2.97 mL of degassed methanol (**1% EDT**). The vials were capped and allowed to stand at room temperature for 20 h, with occasional agitation every few hours. At this time, the supernatant was removed from each vial by pipette, and fresh methanol (10 mL) was added to each vial. The suspensions were allowed to stand at room temperature for 4 h. At this time, each suspension was filtered, and the resulting solids were rinsed with methanol (20 mL), dried briefly under vacuum, and then transferred to separate 10 mL Schlenk flasks. The samples were activated under high vacuum (<100 mTorr) at 180 °C for 24 h. The Schlenk flasks were transferred into a N_2-filled glovebox, and each sample was transferred to a separate glass adsorption tube equipped with a Micromeritics *CheckSeal*. The tubes were removed from the glovebox and the samples were activated for an additional 6 h under high vacuum (<10 µbar) at 180 °C prior to gas adsorption experiments. Surface area data were collected on a Micromeritics 3-Flex gas sorption analyzer using ultrapure N_2 (99.999%) and a liquid N_2 bath. The adsorption results are summarized in Figure S7 and Table S2, and analysis by PXRD in Figure S8 (diffraction data for microcrystalline Zn_2(dobdc) samples were collected on a Rigaku Ultima IV diffractometer equipped with a Cu K_α source).

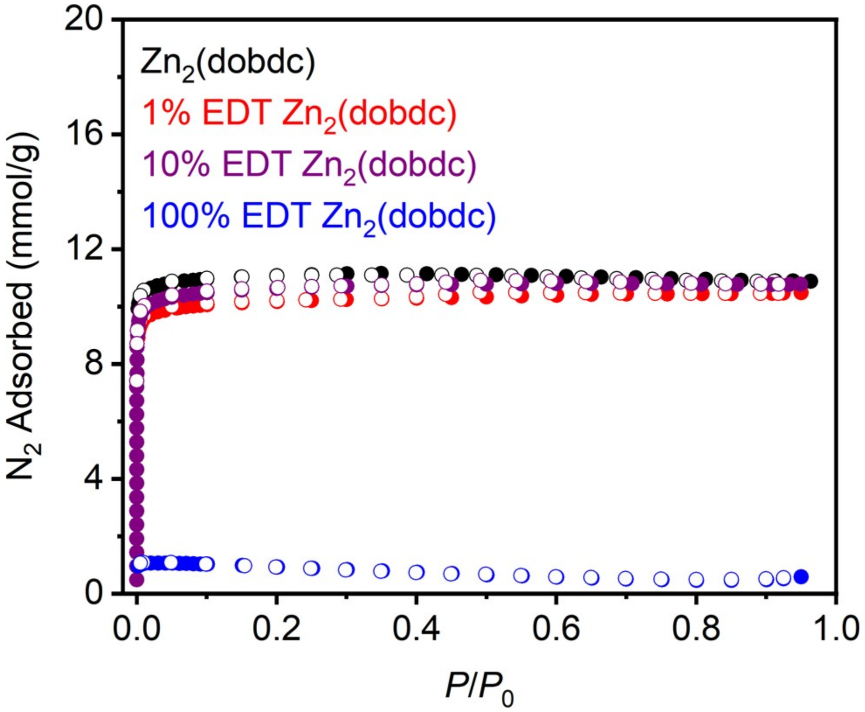

Figure S7. 77 K N_2 adsorption (filled circles) and desorption (empty circles) isotherms of activated, microcrystalline Zn_2(dobdc) as well as activated **1% EDT**, **10% EDT**, and **100% EDT**.

Table S2. Summary of Brunauer–Emmett–Teller (BET) surface areas for microcrystalline Zn_2(dobdc) before and after exposure to solutions of EDT in methanol.

Sample	77 K N_2 BET Surface Area (m^2/g)
Zn_2(dobdc)	1023 ± 1
1% EDT	937 ± 1
10% EDT	962 ± 2
100% EDT	102 ± 1

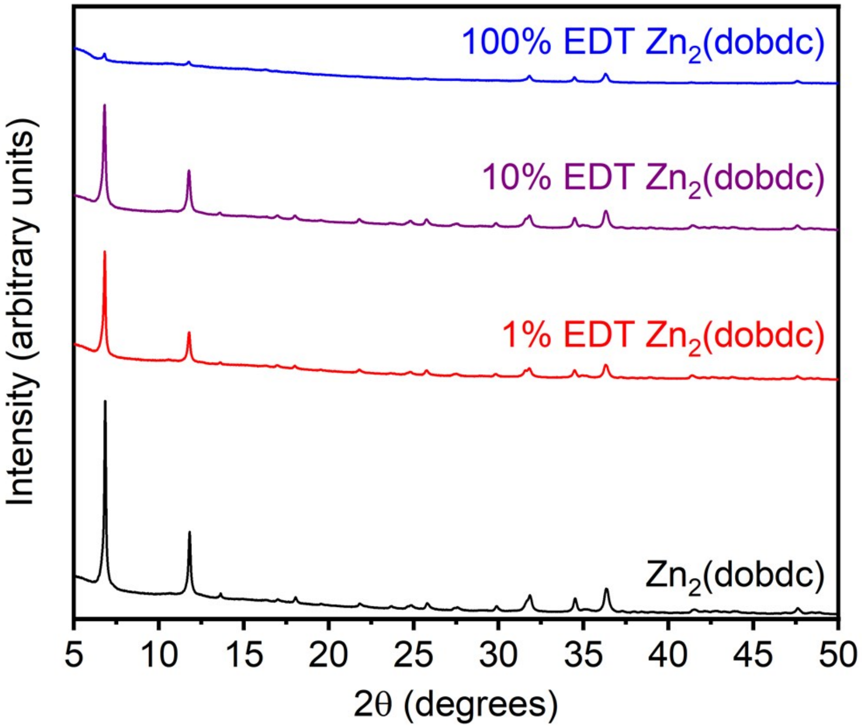

Figure S8. PXRD (λ = 1.5406 Å) patterns of activated, microcrystalline Zn_2(dobdc) as well as activated **1% EDT**, **10% EDT**, and **100% EDT** samples used for gas adsorption analysis. Consistent with the results observed with single-crystalline Zn_2(dobdc), exposure of microcrystalline Zn_2(dobdc) to high concentration solutions of EDT in methanol led to significant amorphization.

6. Scanning Electron Microscopy

The SEM images were obtained using a Leo 1450VPSE variable pressure electron microscope with a LaB_6 tungsten filament electron source. Samples were measured without preparation, such as coating. Images were obtained using a standard Everhart Thornley SE detector, a variable pressure SE detector, and a QBSD solid state backscatter detector.

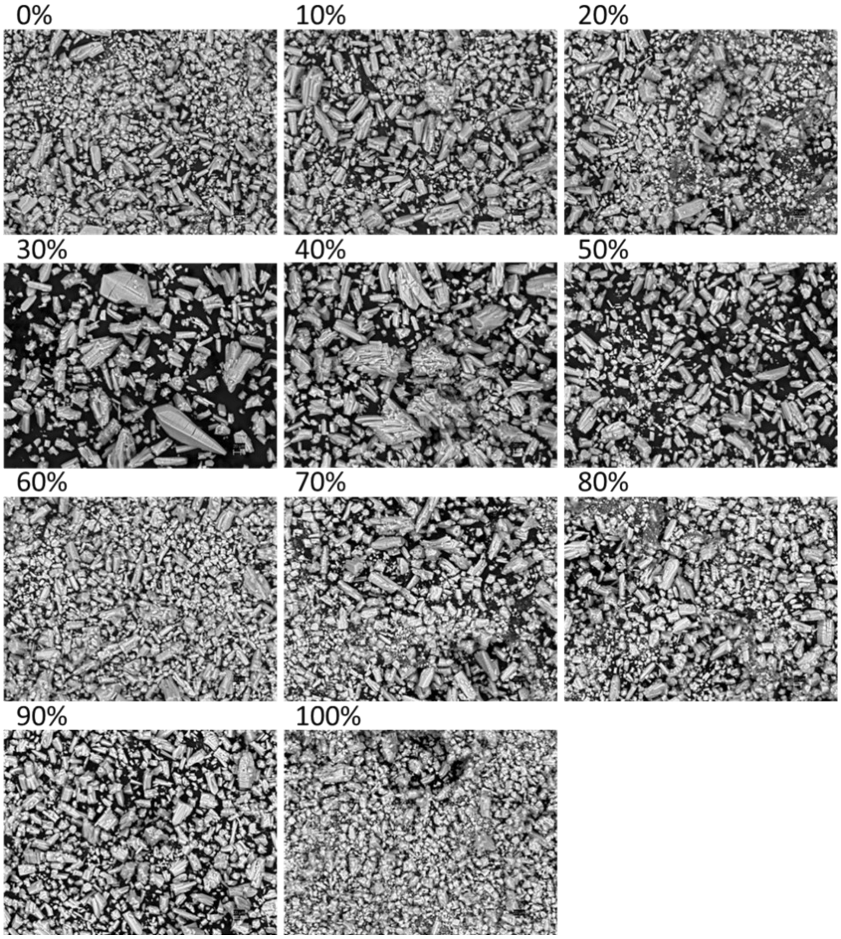

Figure S9. Scanning electron microscopy images of the Zn_2(dobdc) loaded with various amounts of EDT, expressed as mol% of EDT/Zn.

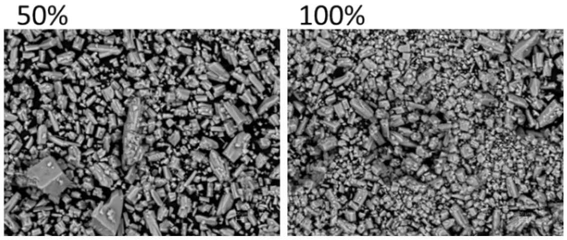

Figure S10. Scanning electron microscopy images of Zn_2(dobdc) loaded with 50% and 100% of nPM, expressed as mol% of nPM/Zn.

7. Theoretical Calculations

As a complement to the experimental work, to provide a better understanding of this highly heterogeneous environment and, at the same time, to enable more in-depth insights into the studied phenomena and their molecular-level origin, we have undertaken a theoretical study of the synthesized compound. Theoretical calculations were carried out at density functional tight binding (DFTB) level of theory, with the DFTB+ code (version 19.1).[9] The "3OB-3-1" set of Slater-Koster parameters (specifically designed for the third-order DFTB methodology – DFTB3) were used for C, H, O,[10] S[11] and Zn[12] atoms. This particular DFTB approach has been specifically parametrized for studying organic and organometallic systems,[10-12] and further on its appropriateness specifically for MOFs was shown as well.[13] Smaller clusters were used to test the possibility for replacement of the $dobdc^{4-}$ ligand by two EDT2- molecules (Figure S11). Large neutral clusters were cut out of the 3D periodic crystal structure of the investigated Zn_2(dobdc), constituted of 1968 atoms in the case which represents the ideal crystal of this compound (Figure S12). Subsequently, clusters with increasing ratio of vacancies were generated by stochastically removing the dithiol molecules. Finally, structures in which the vacancies have been partially filled with methanol molecules were considered as well. Geometry optimizations of all the mentioned clusters were carried out. For the optimized geometries, all possible $(S)H_{dithiol}$…O distances within the clusters were calculated and the corresponding distance histograms were constructed. We hereby pay attention to the histogram segments corresponding to the low R(S)H…O values. As can be seen, our computations suggest that increase of the vacancy concentration leads to enhancement of the ratio of lower R(S)H…O values (i.e. enhancement of the closest (S)H…O contacts). We attribute these finding to the enhanced motional flexibility of the "dangling" SH segments of the coordinated dithiol molecules within the lattice upon sequential removal of dithiol molecules (i.e. as the vacancy content within the cluster increases). This, in turn, enables closer (S)H…O contacts with the acid O atoms. Lower R(S)H…O values, on the other hand, are expected to increase the probability of intermolecular proton transfer (PT) processes from dithiol to acid, thus enabling further motions of the proton via hopping throughout the oxygen centers. Such vacancy-induced enhancement of the PT processes throughout the crystal would govern the observed enhancement of luminescence in the studied system. As a further support to this statement, we have proceeded with optimization of the geometries of the clusters where the protons from the coordinated dithiol S-H groups (the more acidic one) have been transferred to different O-centers within the acid. We have found out that all of these structures (protons located on both carboxylic oxygen or phenolic oxygen atoms) are stable.

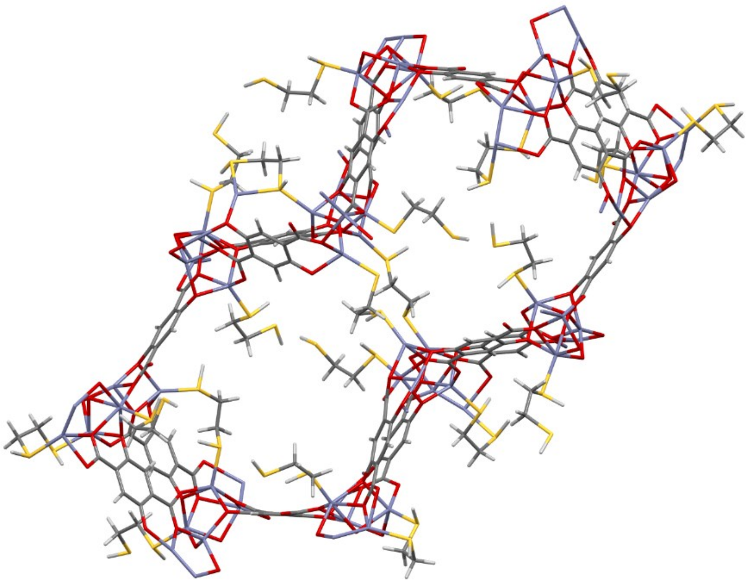

Figure S11. Small cluster of Zn_2(dobdc) were two EDT molecules occupy the position of a single ligand.

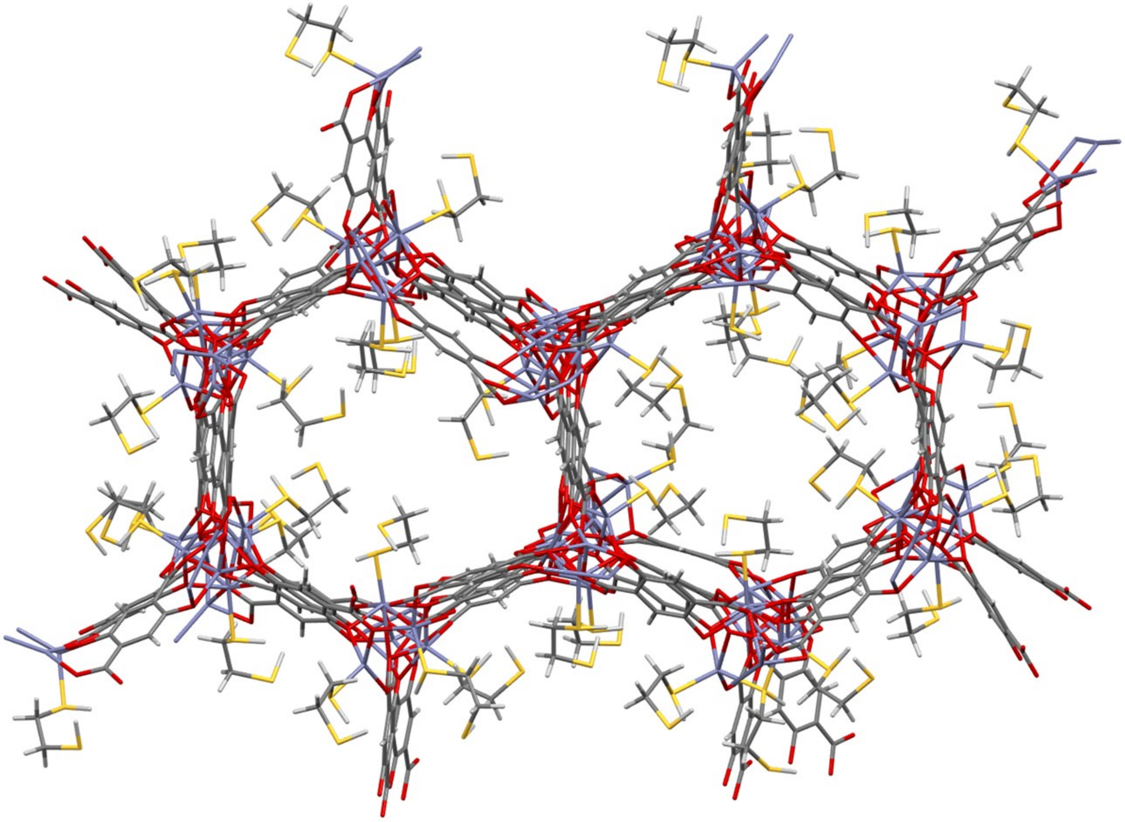

Figure S12. Large cluster of Zn_2(dobdc) with vacancies.

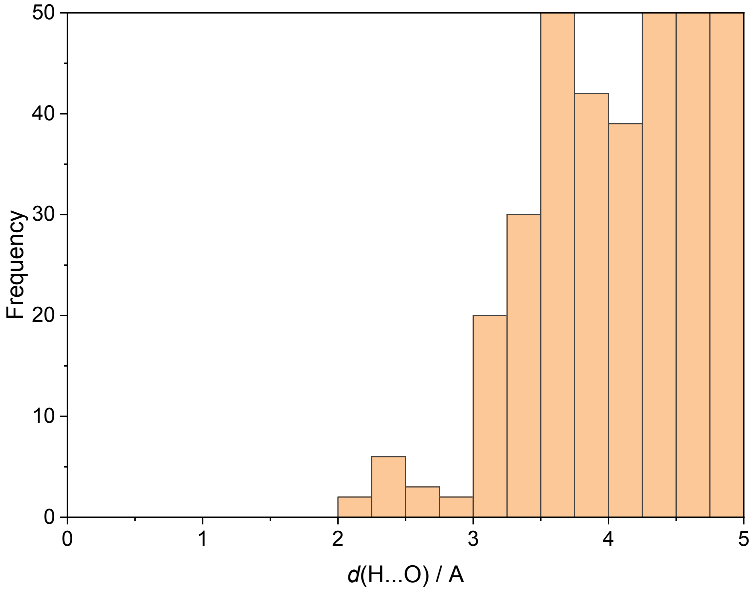

Figure S13. The small-distance segment of the S(H)…O distance distribution histogram for the cluster representing an ideal Zn_2(dobdc) crystal without vacancies.

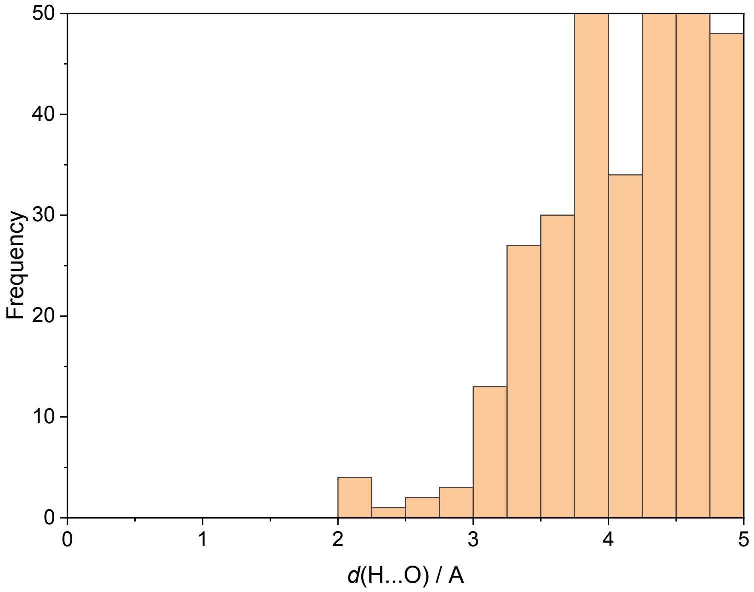

Figure S14. The small-distance segment of the S(H)…O distance distribution histogram for the cluster representing Zn_2(dobdc) crystal with vacancies.

8. Photoluminescence Spectroscopy

Fluorescent emission/excitation spectra were obtained on a Hitachi F-7000 fluorescence spectrophotometer. For each measurement, 2.0 mg of sample was pressed between two glass slides and secured in a sample holder. Photographs of the vials and spectra were collected for MeOH solvated and nPM- and EDT-loaded Zn_2(dobdc) samples are presented in Figure 4 in the main text.

9. Fluorescence Microscopy

9.1. Gradual loading

Slides were prepared by adding approximately 1 mg of crystals to a glass slide which was then sealed with a #1.5 coverslip. The crystals were imaged on an EVOS-fl fluorescence microscope using a DAPI filter cube (λ_{ex} = 357/44 nm, λ_{em} = 447/60 nm) with LED = 70% and integration time = 15 ms through a 40x objective. Three different fields of view were captured for each sample. The acquired images were processed using ImageJ software by converting to 8-bit, adjusting threshold using the "Huang" preset algorithm to create a selection, and then measuring the mean pixel intensity of the selection. Average values for each sample were obtained, and are presented in Figure 4 of the main text, error bars representing standard deviation with n = 3 different fields of imaging. The raw images of EDT and nPM loaded samples are presented in Figure S15 and S16, respectively.

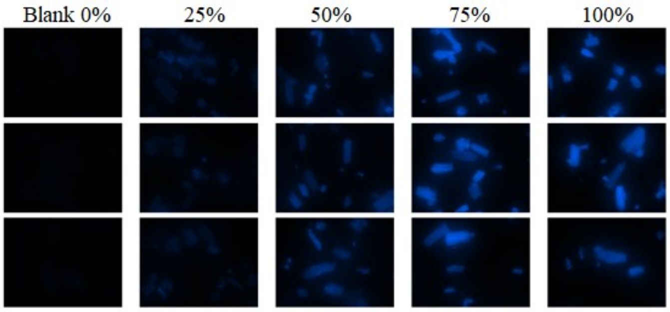

Figure S15. Raw images acquired using EVOS-fl microscope of EDT-loaded Zn_2(dobdc).

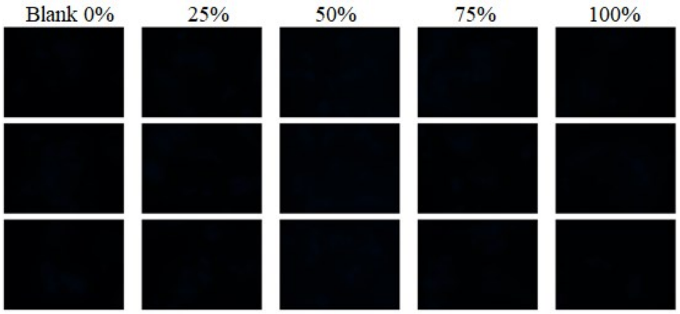

Figure S16. Raw images acquired using EVOS-fl microscope of nPM-loaded Zn_2(dobdc).

9.2. Cation Sensing Screening

Solutions of several metal salts (0.1 M) were prepared using deionized water, including NH_4NO_3, LiCl, $AlCl_3$, $MnCl_2$, $FeSO_4$, $FeCl_3$, $CoCl_2$, $Ni(NO_3)_2$, $Cu(NO_3)_2$, $Zn(NO_3)_2$, $AgNO_3$, $CdCl_2$, $AuCl_3$, $HgCl_2$, and $Pb(NO_3)_2$. Samples (20 mg) of defective-Zn_2(dobdc) (100% EDT/Zn) were transferred to small vials and 1 mL of an aqueous solution was added to each vial. The solutions were soaked for 60 minutes before filtering and washing several times with deionized water. The samples were then dried overnight and characterized by fluorescence microscopy. Approximately 1 mg of crystals was added to each well of a clear-bottom 96-well plate. The sensing procedure was repeated with non-defective Zn_2(dobdc), where the 0.1 M $AlCl_3$ and $FeCl_3$ solutions partially dissolved the crystals.

Fluorescence images were obtained of each well of the plate using a Cytation 5 Bio Tek plate reader (Winooski, VT). The fluorescence imaging detection method was used, and images were set to be captured with zero offset from the center of the well using a 4x PL FL Phase objective, wide FOV setting, and a DAPI filter cube (λex = 377/20 nm, λem = 447/20 nm) with intensity set as LED = 5, integration time = 100, and gain = 0.01. Two independent experiments were conducted, with 6 total wells of each MOF and EDT-MOF sample, with the exception of MOF Al, for which one independent experiment was conducted with 3 total wells. The plates were imaged with clear lids on at room temperature (23–29 °C).

Acquired images were processed using ImageJ software. A stack was created of all the images from the well-plate and the stack was cropped to remove the scalebar. Images in the stack were then processed by converting each to 8-bit, adjusting threshold using the “Huang” preset algorithm to create a selection, and then measuring the intensity of the selection in each image. Images containing contaminants such as dust particles were excluded from the average calculations. Single luminescent crystals in wells C11 and C12 of Plate 1 provided anomalously high mean pixel intensity using the Huang algorithm, so these were also excluded from analysis. Images excluded from average calculations are highlighted in red in Figure S17. Average values are presented in Figure 5 in the main text. Error bars represent standard error over n = 3−6 wells.

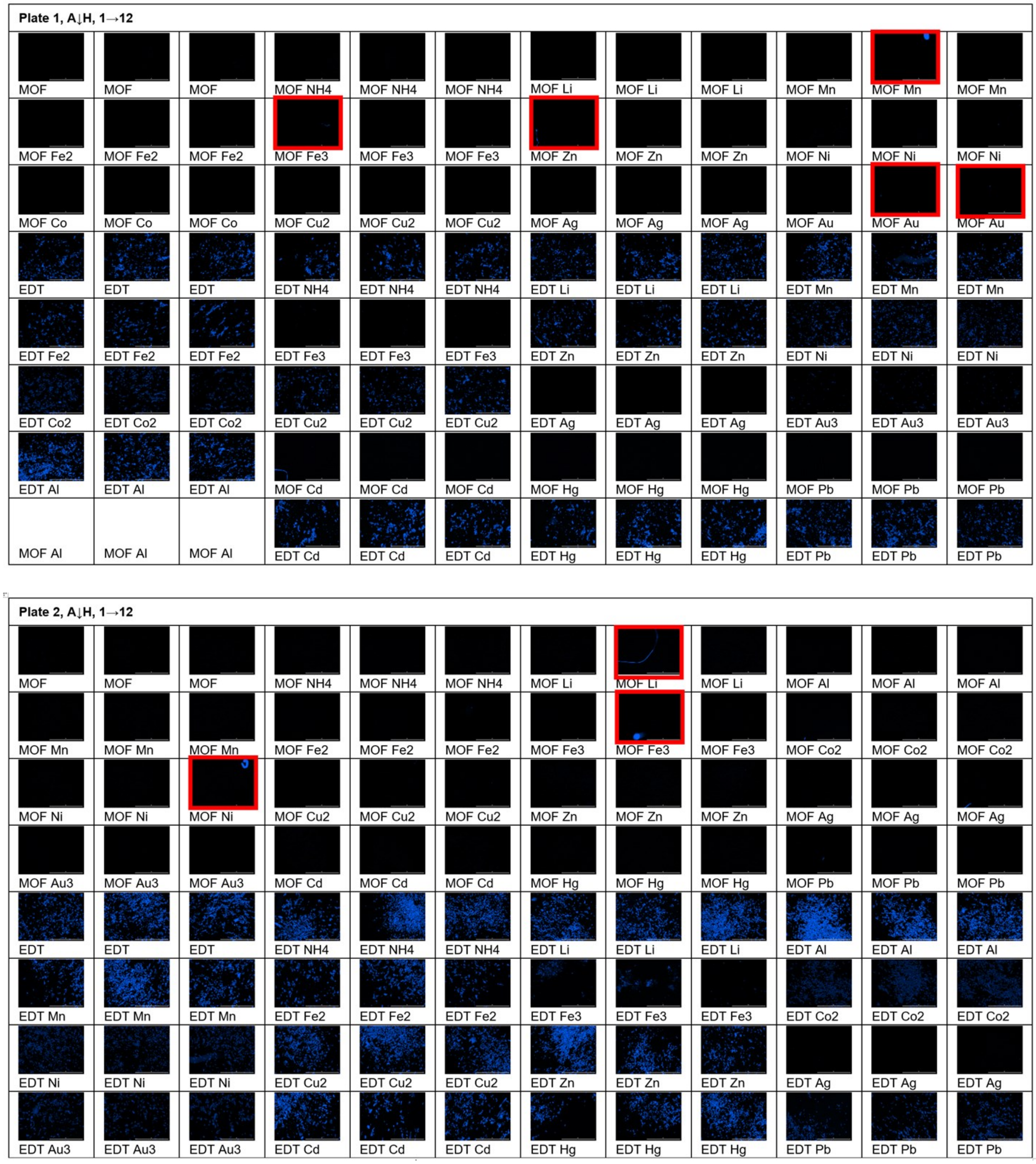

Figure S17. Fluorescence images acquired using BioTek Cytation 5 plate reader.

References

1. S. Cadot, L. Veyre, D. Luneau, D. Farrusseng, E. A. Quadrelli, *J. Mat. Chem. A* **2014**, *2*, 17757-17763.
2. J. L. C. Rowsell, O. M. Yaghi, *J. Am. Chem. Soc.* **2006**, *128*, 1304-1315.
3. M. I. Gonzalez, J. A. Mason, E. D. Bloch, S. J. Teat, K. J. Gagnon, G. Y. Morrison, W. L. Queen, J. R. Long, *Chem. Sci.* **2017**, *8*, 4387-4398.
4. A. A. Coelho, *J. Appl. Cryst.* **2018**, *51*, 210-218.
5. G. S. Pawley, *J. Appl. Crystallogr.* **1981**, *14*, 357-361.
6. Y. G. Andreev, G. S. MacGlashan, P. G. Bruce, *Phys. Rev. B: Condens. Matter Mater. Phys.* **1997**, *55*, 12011-12017.
7. H. M. Rietveld, *J. Appl. Cryst.* **1969**, *2*, 65-71.
8. M. I. Gonzalez, M. T. Kapelewski, E. D. Bloch, P. J. Milner, D. A. Reed, M. R. Hudson, J. A. Mason, G. Barin, C. M. Brown, J. R. Long, *J. Am. Chem. Soc.* **2018**, *140*, 3412-3422.
9. B. Hourahine, B. Aradi, V. Blum, F. Bonafé, A. Buccheri, C. Camacho, C. Cevallos, M. Y. Deshaye, T. Dumitric, A. Dominguez, S. Ehlert, M. Elstner, T. vander Heide, J. Hermann, S. Irle, J. J. Kranz, C. Köhler, T. Kowalczyk, T. Kubar, I. S. Lee, V. Lutsker, R. J. Maurer, S. K. Min, I. Mitchell, C. Negre, T. A. Niehaus, A. M. N. Niklasson, A. J. Page, A. Pecchia, G. Penazzi, M. P. Persson, J. Rezác, C. G. Sánchez, M. Sternberg, M. Stöhr, F. Stuckenberg, A. Tkatchenko, V. W.-z. Yu, T. Frauenheim, *J. Chem. Phys.* **2020**, 152, 124101 (1-19).
10. M. Gaus, A. Goez, M. Elstner, *J. Chem. Theory Comput.* **2013**, *9*, 338-354.
11. M. Gaus, X. Lu, M. Elstner, Q. Cui, *J. Chem. Theory Comput.* **2014**, *10*, 1518-1537.
12. X. Lu, M. Gaus, M. Elstner, Q. Cui, *J. Phys. Chem. B* **2015**, *119*, 1062-1082.
13. E. Jin, I. S. Lee, D. Kim, H. Lee, W-D. Jang, M. S. Lah, S. K. Min, W. Choe, *Sci. Adv.* **2019**, *5*, eaav4119 (1-8).